Results in Physics 5 (2015) 62–68

Contents lists available at ScienceDirect

Results in Physics

journal homepage: www.journals.elsevier.com/results-in-physics

Exploring new frontiers in the pulsed power laboratory: Recent progress

S. Adamenko [a,b], A. Esaulov [a,*], B. Ulmen [a], V. Novikov [a], S. Ponomarev [b], A. Adamenko [b], V. Artyuh [b], A. Gurin [b], V. Prokopenko [b], V. Kolomiyets [b], V. Belous [b], K.-J. Kim [a,c], G. Miley [a,c], A. Bassuney [a], D. Novikov [a]

[a] Proton Scientific Inc., 402 N. Maple St, Urbana, IL 61802, USA
[b] Proton-21 Electrodynamics Laboratory, 2 Moldavskaya St Suite 67, Kiev 03057, Ukraine
[c] Department of Nuclear, Plasma and Radiological Engineering, University of Illinois, 216 Talbot Laboratory, MC-234, 104 S. Wright St, Urbana, IL 61801, USA

ARTICLE INFO

Article history:
Received 23 December 2014
Accepted 25 February 2015
Available online 2 March 2015

Keywords:
Pulsed power
Electron beam
Collective nuclear effects
Material analysis

ABSTRACT

One of the most fundamental processes in the Universe, nucleosynthesis of elements drives energy production in stars as well as the creation of all atoms heavier than hydrogen. To harness this process and open new ways for energy production, we must recreate some of the extreme conditions in which it occurs. We present results of experiments using a pulsed power facility to induce collective nuclear interactions producing stable nuclei of virtually every element in the periodic table. A high-power electron beam pulse striking a small metallic target is used to create the extreme dynamic environment. Material analysis studies detect an anomalously high presence of new chemical elements in the remnants of the exploded target supporting theoretical conjectures of the experiment. These results provide strong motivation to continue our research looking for additional proofs that heavy element nucleosynthesis is possible in pulsed power laboratory.

1. Introduction

Nuclear fusion processes that drive energy production in stars as well as the creation of nuclei as heavy as iron and nickel [1,2] are understood well enough to start conceptual designs of new types of power plants to harness some of these processes [3,4]. Fusion reactions in star interiors as well as those in hot plasma generated in the laboratory environment are based on mechanisms of pair-collision of the reacting nuclei, when their kinetic energy is high enough to tunnel through the Coulomb barrier and engage in strong nuclear interactions.

At the same time, even a theoretical concept of processes in the Universe responsible for the production of nuclei heavier than iron and nickel is incomplete [5–7]. Like fusion models, current models of heavy element nucleosynthesis are based on pair-collision mechanisms involving a capture of free neutrons by target nuclei which then undergo β^- decay moving to higher atomic numbers in the periodic table [8]. Relatively slow neutron capture is called the s-process and takes place in the stable interiors of the massive (several solar masses) stars on time scales ranging from ten million to a few billion years.

Yet if we consider the observed isotope composition of the Universe [9] the model of s-process alone can only explain the abundances of about half of heavy isotopes [10]. Creation of the remaining isotopes is currently attributed to other pair-collision-type processes with the largest contribution by the rapid neutron capture or the r-process, which is theorized to occur solely in type II, core collapse supernovae [6–8,10] on much shorter time scales of a few seconds. R-process models of different levels of sophistication have been constructed over the years, yet unanswered questions are by far more numerous than solved problems [10].

Some answers to numerous unresolved issues in heavy element nucleosynthesis may be found in alternative theories and models. One of these models is the concept of collective nuclear interactions that suggests a nucleosynthesis mechanism occurring on a very short time scale. According to this concept, collective nuclear interactions may be triggered by simultaneous acceleration of all particles in the system. If amplitude and coherency of the acceleration are high enough, these factors may significantly increase the transparency of Coulomb barrier [11]. In this case contrary to pair collisions the strong interactions will be engaged not just between two reacting nuclei but throughout large ensembles of nuclei, which will form heavy nuclear clusters as a result of system self-organization [12,13].

In any finite volume such coherent particle acceleration cannot be sustained indefinitely. Once the acceleration starts to drop these heavy nuclear clusters become unstable and decay into various stable isotopes. Unlike pair-collision nuclear reactions that are

* Corresponding author.

http://dx.doi.org/10.1016/j.rinp.2015.02.005
2211-3797/

characterized by specific nuclear products, the nuclear transmutation process driven by the collective interactions produces stable isotopes of virtually every element in the periodic table.

Most of the matter in Universe exists in a state of thermal equilibrium or quasi-equilibrium, which is signified by random particle acceleration. Shock waves that restore thermal equilibrium in the media cannot create the conditions required for coherent particle acceleration for the same reason. Coherent acceleration, however, can be achieved by an action of a long range force, which can be either gravitational or electromagnetic force. In the former case a possible site for such process is type II supernova during its core collapse driven by strong gravitational field of the dying star [14]. It is remarkable that this potential site for collective nuclear interaction process is very close in time and location with the site for the r-process.

The electromagnetic force can also create an environment for coherent acceleration of ions. A radiative collapse of z-pinch [15] is one of the mechanisms that could serve this goal. However, in our research we utilize the effect of an electron beam channel collapse induced by electron beam–solid target interaction and beam self-focusing in the dense plasma [16,17] of the resultant virtual electrodes [18].

In this paper we describe a pulsed power laboratory experiment to test the concept of collective nuclear interactions using a high-power, nanosecond-scale electron beam pulse striking a small metallic target. A material analysis study shows anomalously high concentrations of new chemical elements that are present in the remnants of the exploded target. These elements are spread across the board of the periodic table and are detected in the amounts consistent with energy balance estimations, assuming that they were formed from the original target material.

2. Pulsed power device and the experimental setup

While a manipulation of gravitational field is unattainable in the laboratory, another type of long-range interaction due to the electromagnetic force can be reproducibly generated and controlled in a pulsed power device. Among a variety of pulsed power configurations, an electron beam setup has been selected for its ability to deliver the electromagnetic energy in a single short pulse into a relatively small volume along the central channel of the target producing extremely dense plasma.

We report the results of experiments at our pulsed-power facility IVR-1 in Kiev, Ukraine that uses a 0.5 MV generator producing a 40 kA, 20 ns electron beam pulse to strike a sub-millimeter anode target. The principal scheme of the high voltage pulsed power device and its simplified electric circuit schematic is shown in Figs. 1 and 2A.

The primary features of the pulsed power device are the capacitor energy source, the vacuum inductive storage system, the set of plasma erosion opening switches (PEOS) and the relativistic vacuum diode (RVD). The vacuum systems of the RVD chamber and the inductive storage are combined and maintained at a base pressure of $<5 \times 10^{-5}$ Torr during the shot. The primary function of the pulsed power device is to shape and compress the voltage pulse from the main 3 μF capacitor charged to 50 kV (3.75 kJ stored energy). Pulse compression is performed by an array of twelve plasma opening switches [19–21] axially-arranged around a solid central conductor (cathode) and operated from a separate capacitor bank (see Fig. 2A).

After the main capacitor and PEOS capacitor bank are charged with negative polarity, the spark gap switch for the PEOS is triggered and plasma is generated in the gap between the vacuum inductive storage system and the grounded outer chamber anode, creating a low-resistance short circuit bridge. A few microseconds later, the spark gap for the main capacitor is triggered. The capacitor starts to discharge accelerating current in the vacuum inductive storage system through the short circuit bridge to the ground sustained by plasma in the PEOS region.

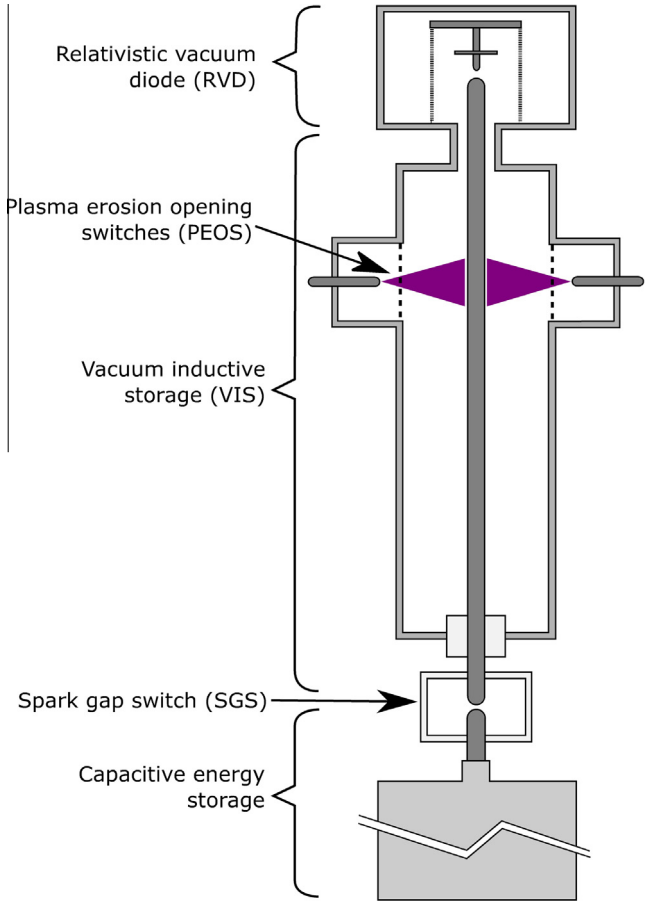

Fig. 1. Schematic of the electron beam pulsed power device.

An additional microsecond later, the resistance of the plasma bridge in the PEOS region abruptly rises by orders of magnitude on a nanosecond time scale, effectively disconnecting the short circuit plasma bridge. The inductively stored energy is promptly delivered to the RVD inducing a very narrow, ~20 ns, ~0.5 MV voltage spike (see Fig. 2B). The generated electron beam is relativistic with electron velocities ~0.86 c ($\gamma \approx 2$) and estimated peak power up to 12 GW.

The assembly of the RVD [12] is shown in Fig. 3. The anode of the RVD (Fig. 3A) is a cylindrically shaped target with a smooth semi-spherical top, which protrudes through the center of an accumulating screen (Fig. 3B). The electron beam is focused at the tip of the anode target (Fig. 3C) causing the target to explode and "peel open" forming a deep axial channel (Fig. 3D) while ejecting a significant part of the target material on the accumulating screen (Fig. 2E). The cathode plate, the anode target, and the accumulating screen were fabricated from ultra-pure copper (99.9999% metals basis purity, Alfa-Aesar).

3. Material analysis of accumulating screens

According to the concept of the transmutations produced by the collective nuclear interactions, various elements should be generated in detectable amounts from the break-up of the heavy nuclear clusters. We undertook material analysis of the target explosion particles in order to directly examine the products of the

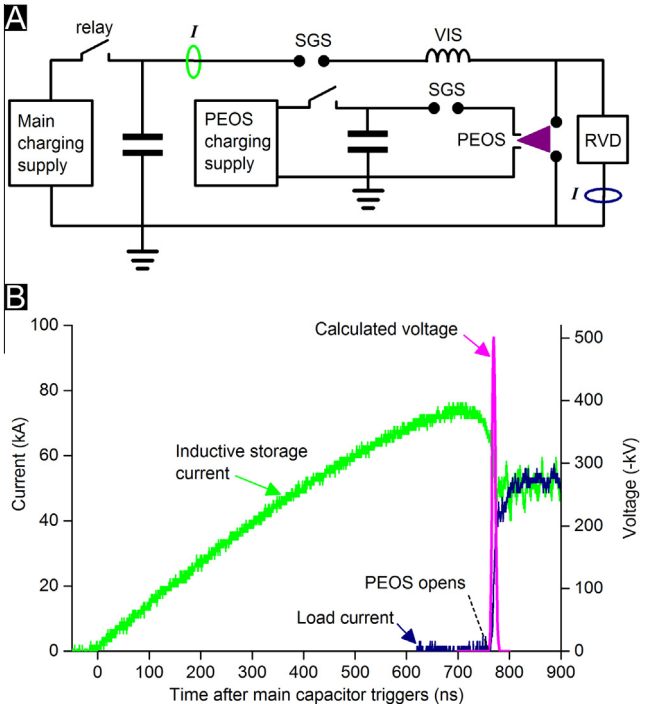

Fig. 2. Electron beam pulsed power device with (A) basic electrical circuit diagram and (B) a typical trace of the current in the inductive storage and the load current *I*, measured by two Rogowski coils (green and navy ovals in the plot B), given with the estimated voltage between the electrodes of the discharge chamber. (For interpretation of the references to colour in this figure legend, the reader is referred to the web version of this article.)

transmutation process. The high purity of the anode target and accumulating screen allows minimizing the background signal accurately distinguishing newly created element from the original impurities in the matrix material. Examination of the accumulating screens was performed using two techniques: energy dispersive X-ray spectroscopy (EDS) was performed in our laboratories and glow discharge mass spectroscopy (GDMS) was independently performed by Evans Analytical Group.

The EDS analysis was performed on surface of an accumulating screen by searching for micrometer-scale particles that stand out against the copper matrix background by using contrast techniques with the backscatter and secondary electron detectors. The lower limit of the EDS detection is about 1–2%, so only particles with a significant concentration of a given element can be detected. This introduces a human factor when selecting candidate particles based on the differential contrast, explaining the lower success rate in finding particles containing elements detected in low concentrations by GDMS such as silver and europium. About 25% of the selected particles showed only copper X-ray peaks (along with an expected small amount of oxygen always present from surface oxidation). When a particle of interest was located, an X-ray spectrum was collected for two minutes using a 20 keV electron beam accelerating voltage. The sample surface was divided into 7 concentric rings spaced radially by 1 mm. The analysis areas within each ring were evenly spaced as shown in Fig. 4A. The areas themselves were squares of 0.36×0.36 mm with $\sim$3 μm probing depth, and the number of the analysis areas per ring was chosen in order to analyze at least 5% of the total area of each ring.

EDS was used to directly examine individual particles of the exploded target remaining on the surface of the accumulating screen for their elemental composition. A detailed analysis of one typical screen resulted in 741 captured spectra of individual particles (Fig. 4). Hundreds of other screens examined by EDS in less exhaustive surveys corroborate the composition of the elements shown here.

Only particles with significant concentrations of non-matrix elements show peaks using EDS because of the 1–2% detection threshold. Because of the relatively large penetration depth of the EDS probe, in order to find elements above the threshold concentration, only particles of the size not less than approximately half micron in diameter were examined. It is unlikely that such large particles could be produced directly by a plasma deposition process. At the same time, the size and shape of the particles shown in the scanning electron microscope (SEM) images (Fig. 4B and C) indicate a liquid phase deposition consistent with particles coming from the molten interior of the target during the explosion in the direction from the center of the screen toward its periphery (Fig. 4A–C). Control screens, which were not exposed to the explosion, are all of uniform contrast in SEM as expected of the high purity copper matrix with all original impurities considerably under the limit of EDS detection.

GDMS is the best available technique for an accurate quantitative comparison of low concentrations of elements in copper matrix films [22] and was used to measure and compare

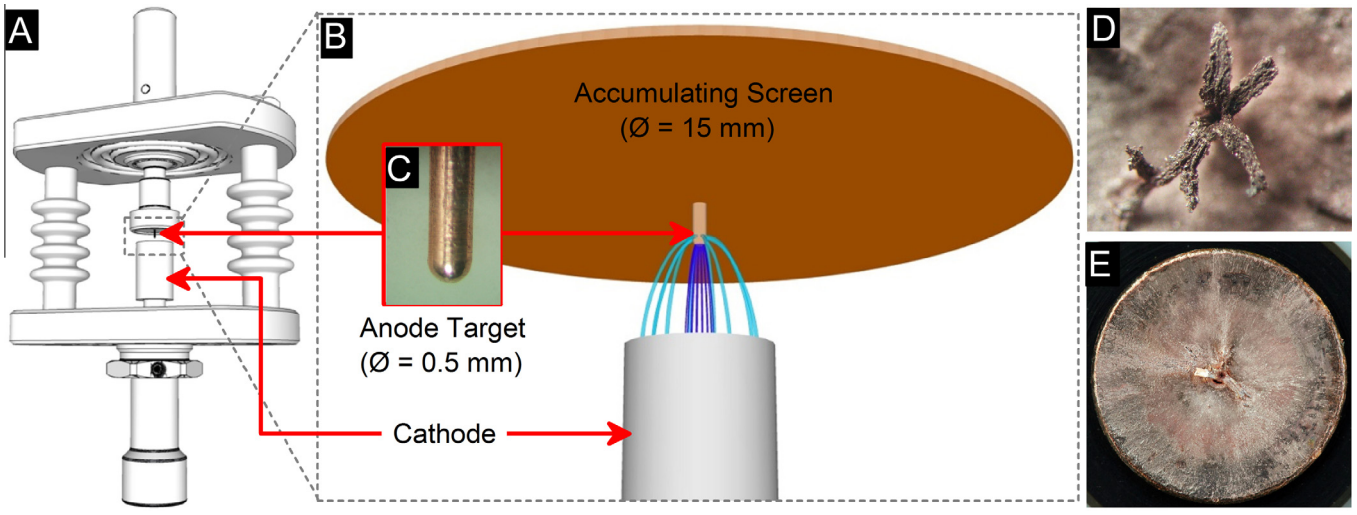

Fig. 3. Schematic and photographs of the diode assembly. The 3-D schematic of the diode is shown (A) with a focus on the accumulating screen and (B) anode target. (C) A zoomed photograph shows the tip of the copper anode target and (D) a typical exploded target. (E) A photograph of an exploded target with the accumulating screen shows the deposition of the anode target ejecta, which was subject to the material analysis.

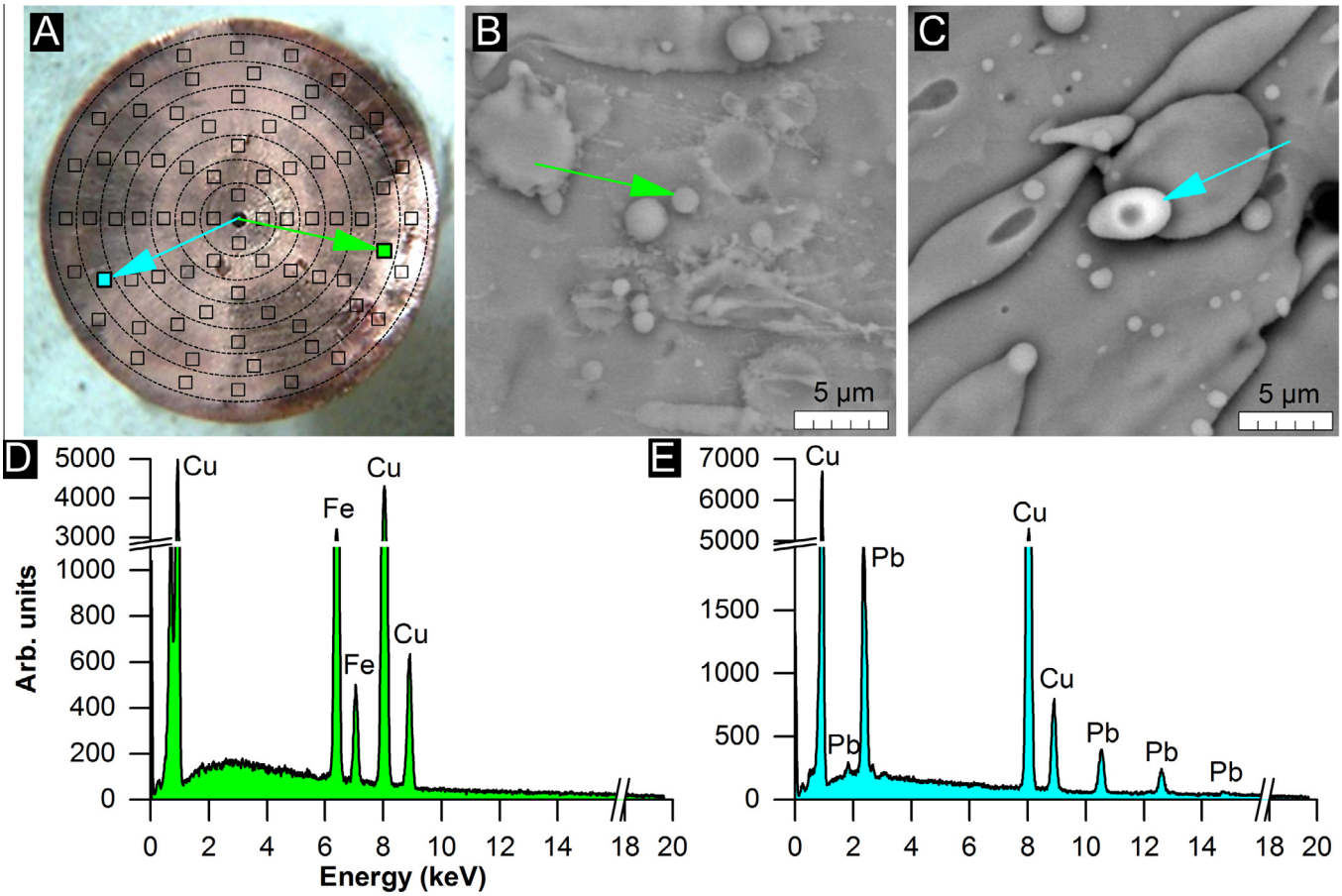

Fig. 4. Exploded target material analysis. (A) A schematic indicates the sites (black squares) for EDS analysis on the copper accumulating screen. (B) Scanning electron microscope micrographs of an iron-containing particle and a (C) lead-containing particle. The arrow points toward the particle of interest as well as indicates the deposition direction from the anode target explosion. (D) The X-ray EDS spectra of the iron particle and (E) lead particle show characteristic peaks for only a single metallic element (besides the copper matrix).

concentrations of select products of the exploded target on the accumulating screens. We worked closely with Evans Analytical Group (Liverpool, NY) to perform the GDMS analysis on our samples. First, the baseline was tested on the 99.9999% metals basis purity copper foil (Alfa Aesar), the material from which all accumulating screens, anode targets, and cathode cover plates were fabricated. The control measurements of the foil showed only Al, S, and Fe in concentrations above the lower limit of quantification (LOQ) [teal lines in Fig. 6] while the concentrations of these elements on the screens after the experiments were more than an order of magnitude higher.

The next step analyzing the accumulating screens was to determine the film thickness of the deposited target material by measuring a depth profile of a single element, in this case iron. Because GDMS elemental measurements are performed in sequence, the known depth profile allowed an estimation of how many elements could be measured inside the film of the certain thickness and how we should compute the error range of the concentrations with respect to the order in which the elements were scanned. Iron was chosen because particles containing large concentrations of iron were detected using EDS and the trace concentration was reported on the manufacturer's certificate of the copper foil. The burn depth at each sample point was estimated based on the known sputter rate for a flat copper sample to compensate for the roughness of the accumulating screen surface. The true total burn depth was estimated at between 5 μm and 10 μm and the midpoint value of 7.5 μm is used in Fig. 5. The sample roughness did not affect the measurement error of the concentrations which varies across samples by ~20%, or the accuracy typically within a factor of 2 of the true value.

In the depth profiling GDMS technique, there were a limited number of elements that we could examine in this small film thickness. For all experiment screens we detected 11 out of the 25 selected elements and they displayed a consistent trend exponentially decreasing concentration with increasing depth of the probe. The depth profiles from a typical screen are presented in Fig. 5. The maximum concentrations of these elements were significantly above the baseline measurements for all samples. The estimated masses of the elements on a screen surface are given in Table 1.

All potential sources of contamination in the discharge chamber are alloys, such as stainless steel. Their contribution to the material deposition on screen would be picked up by GDMS analysis and signified by sharp peaks of base elements of these alloys such as iron and chromium over the rest of elements.

Thus, we consider the interior of the exploded anode target to be the main source of the material deposition on a surface of accumulating screen. Results of material analysis corroborate our theoretical concept of pulsed power initiated nucleosynthesis.

4. Discussion

Pulsed power devices, like the world's most powerful X-ray source Z-Machine at Sandia National Laboratory [23], are known to generate extreme plasma conditions. We chose an electron beam as a driver to trigger collective nuclear effects through coherent particle acceleration because of extreme pulse compression

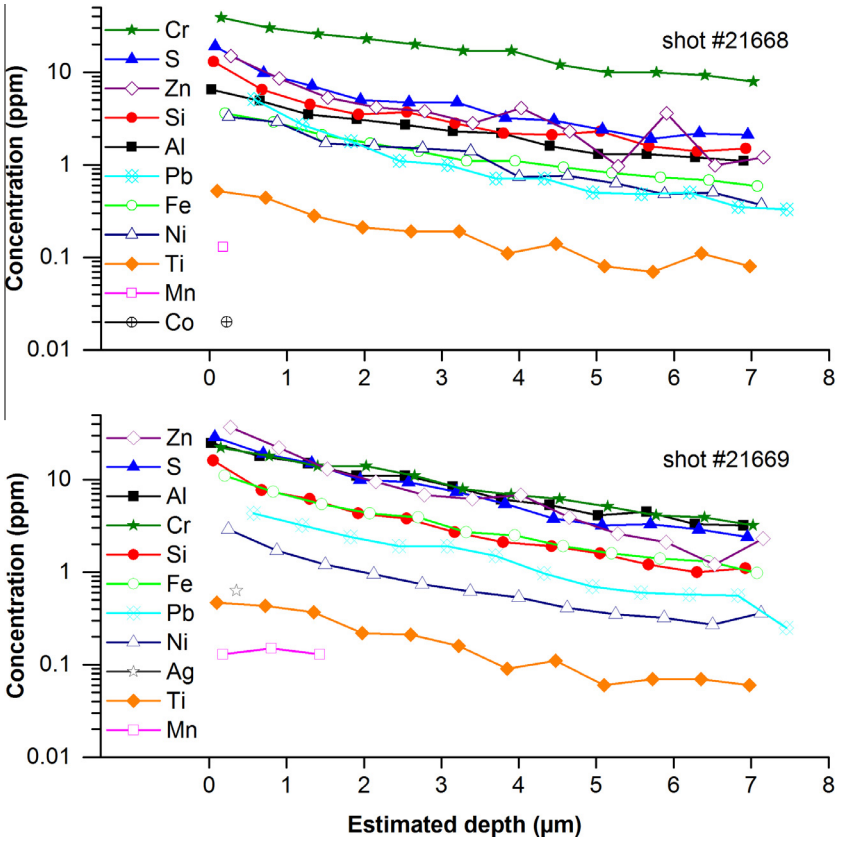

Fig. 5. Material analysis of the exploded targets in shots 21,668 and 21,669. The GDMS depth profiles show an exponential decrease in the elemental concentrations measured over ~7 μm depth.

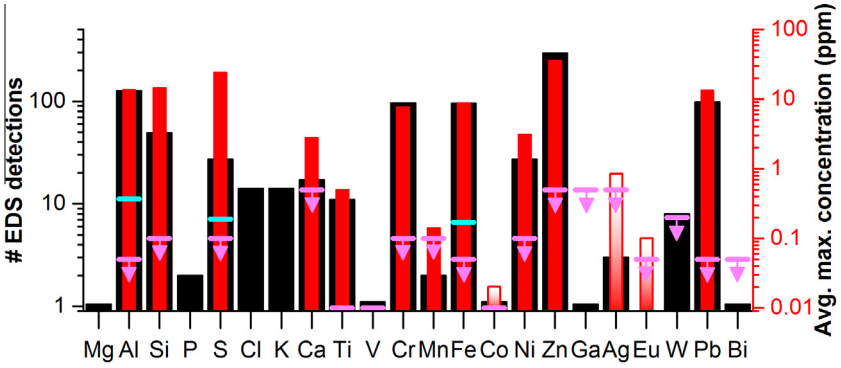

Fig. 6. Exploded target material analysis. The EDS particle count (left axis, black bars) shows good general agreement with the GDMS maximum concentrations averaged over all samples (right axis, red bars): the abundances of elements estimated by EDS match their concentrations measured by GDMS. Cobalt, silver and europium are shown as a gradient to indicate that only some of the samples had their concentrations above the limit of quantification. The teal lines indicate measurements of the baseline material. For elements where the line is not present the baseline concentration was below the limit of quantification (magenta arrows). (For interpretation of the references to colour in this figure legend, the reader is referred to the web version of this article.)

Table 1
Atomic numbers Z and rough estimations of total masses M of the elements detected on a surface of accumulating screen according to the GDMS data shown in Fig. 5A.

	Al	Si	S	Ti	Cr	Mn	Fe	Ni	Zn	Ag	Pb
Z	13	14	16	22	24	25	26	28	30	47	82
M (ng)	~40	~15	~40	~1.5	~80	~0.5	~30	~10	~100	~1.5	~60

that can be achieved on a scale of <10 ns. Current accelerators in most z-pinch experiments provide a significantly longer rise time of $\geqslant$100 ns. Another principal advantage of using the electron beam driver is due to an effect of beam self-focusing that allows delivering a significant amount of energy into a relatively small volume. This feature in our experiments manifests in a "hole boring" effect leaving a narrow channel along the central axis of the remains of anode target.

Electron beam power deposition per unit area P_b can roughly be estimated at lower bound assuming beam diameter, d_b, to be a diameter of the axial channel in the anode target ~150 μm, which results in $P_b \approx 1$ TW/mm^2. Upper bound of this estimation may assume the beam diameter equal to the size of a single electron beam filament $d_b \leqslant 1$ μm. This value has been suggested by particle-in-cell (PIC) kinetic modeling of the relativistic electron beam propagation through dense plasma [16,17]. Simulation with another PIC code in the diode geometry close to one in our experiments [24] suggests beam self-focusing to a diameter 50 μm that results in power densities $P_b \approx 10$ TW/mm^2.

For comparison, the power density level 10 TW/mm^2 was considered to be relevant in the electron beam fusion concept [18]. Achieving this level for the whole area of the fusion target ~1 cm^2 was problematic even at largest pulsed power facilities, such as the Particle Beam Fusion Accelerator-II (PBFA-II) [25]. In the latter case the light ion beam source has been implemented to get rid of intrinsic restrictions of relativistic electron beam and to increase the power density that can be delivered to the target up to the values 0.5–1 TW/mm^2.

Delivery of high energy density to the target region by the pulsed device was additionally confirmed in experiments with similar targets, in which Thomson analyzer had been used to register near-MeV protons and deuterons [26] as well as up to 2 MeV α-particles [27]. In the latter case the p-^{11}B (proton-boron) nuclear reaction had been ignited to source α-particles. Note that the temperature required to ignite the p-^{11}B reaction is almost ten times higher than that for D-T fusion reaction.

In the concept of collective nucleosynthesis the key parameter is the value of coherent particle acceleration. The peak value of this parameter in our experiment is mostly defined by the minimum diameter of the electron beam and by the beam current. Using the values 50 μm and 28 kA (limiting Alfven current value for the conditions of our experiment), an order of magnitude upper bound estimate suggests that this value can exceed 10^{11} m/s^2. 1D modeling of type II Supernova [14] yields the inward acceleration ~5×10^9 m/s^2 at the core collapse stage. Although the temperatures and densities of Supernova interior are unattainable in the laboratory environment, some of the parameters such as the ion acceleration can be matched in experiment even at mid-level pulsed power facilities.

We expect that nuclear transmutations produce predominantly stable isotopes, particularly the ones with the lowest binding energies. Light nuclei that are composed of alpha particles are called α-conjugate nuclei [28], they have an even and equal number of protons and neutrons and are characterized by enhanced nuclear bonding. This effect of enhanced nuclear bonding for α-conjugate nuclei also extends to heavier nuclei, which are more complex nuclear systems represented by α-clusters and additional valence neutrons [29]. In Table 1 we observe significant concentrations of the metals of iron group (from Ti to Zn) with enhanced nuclear bonding, which nuclei have an even number of protons. On the other hand, measured concentrations of the iron group metals that have an odd number of protons, such as V, Mn and Co are either below or only slightly above their limit of quantification (LOQ) values.

In our experiments the matrix material for nuclear transmutations is copper, the element which has one of the highest binding energies per nucleon. Then, the transmutation process is likely to demand an external energy input. Using data in the Table 1, estimations by order of magnitude show that this energy demand is consistent with the expected energy input to the target $\geqslant$100 J. This energy balance consideration suggests the amount of transmuted material should rise linearly with the increase of input energy.

A new electron beam pulsed power facility IVR-3 was recently opened in Urbana, Illinois. The IVR-3 device is an upgraded version of IVR-1 device with capability of increasing the charging voltage of main capacitor up to 100 kV. Variation of this parameter in the range 50–65 kV will not require an essential hardware adjustment and will be a goal of new series of experiments to study the effects due to scaling up the input energy and beam current.

However, it is possible that the material analysis techniques that we described in this paper may not be accurate enough to quantify the effects due to input energy scaling in the above parameter range. We also anticipate some difficulties simply extending our experimental design to a larger pulsed power facility. There are some negative factors that can diminish particle acceleration as we move toward higher currents. Decreasing efficiency of pulse compression by PEOS [30] as well as less efficient self-focusing of the electron beam due to beam splitting into multiple filaments, each carrying an Alfven current [16,17] are among these negative factors.

In order to counteract these issues in the new Urbana laboratory, in addition to material analysis we shall also focus on investigating other aspects of nucleosynthesis. This research will include detection and energy spectrum measurements of protons, neutrons and other high-energy particles as well as the X-ray and γ-photons that can potentially turn transmutation process into an energy production mechanism.

5. Conclusion

This work presents results of novel experiments using a pulsed power facility to induce collective nuclear interactions by creating an extreme dynamic environment of coherent particle acceleration. We expected that the initiated nuclear transmutations would produce stable nuclei of virtually every element in the periodic table, placing these processes beyond any known type of nuclear reactions. We have demonstrated in experiments that these elements are generated in the amounts that are significant enough to be detected and measured by conventional material analysis methods.

The results presented here suggest that collective nucleosynthesis producing various chemical elements may be feasible in a laboratory environment, although further a systematic study of this process using additional diagnostic methods, such as neutron and γ-ray detection, is required. Upgraded pulsed power equipment with added diagnostics in our Illinois facility will allow continued experiments gaining deeper insights into the nature of this process.

Acknowledgments

The authors would like to acknowledge helpful comments in preparing this manuscript from J. P. VanDevender, T. J. Dolan, and A. J. Leggett. We thank the engineers and technical staff at Proton-21 Electrodynamics Laboratory in Kiev, Ukraine and Nick Boyea and the team at Evans Analytical Group Laboratories in Liverpool, NY for their work on the GDMS measurements.

References

[1] Bethe HA. Energy production in stars. Phys Rev 1939;55:434–56.
[2] Burbidge KM, Burbidge GR, Fowler WA, Hoyle F. Synthesis of the elements in stars. Rev Mod Phys 1957;29:547–650.
[3] Rebut P-H. ITER: the first experimental fusion reactor. Fusion Eng Des 1995;30:85–118.
[4] Miller GH, Moses EI, Wuest CR. The national ignition facility. Opt Eng 2004;43:2841–53.

[5] Hillebrandt W. The rapid neutron-capture process and the synthesis of heavy and neutron-rich elements. Space Sci Rev 1978;21:639702.
[6] Cowan JJ, Cameron AGW, Truran JW. R-process nucleosynthesis in dynamic helium-burning environments. Astrophys J 1985;294:656662.
[7] Mathews GJ, Cowan JJ. New insights into the astrophysical r-process. Nature 1990;345:491494.
[8] Sneden C, Cowan JJ. Genesis of the heaviest elements in the Milky Way galaxy. Science 2003;299:70–5.
[9] Lodders K. Solar system abundances and condensation temperatures of the elements. Astrophys J 2003;591:12201247.
[10] Arnould M, Goriely S, Takahashi K. The r-process of stellar nucleosynthesis: astrophysics and nuclear physics achievements and mysteries. Phys Rep 2007;450:97–213.
[11] Vysotskii VI, Adamenko SV. Correlated states of interacting particles and problems of the Coulomb barrier transparency at low energies in nonstationary systems. Tech Phys 2010;55:613621.
[12] Adamenko SV. Method and device for compressing a substance by impact and plasma cathode, International Patent EP1464210 B1, 27 September 2006.
[13] Novikov V, Kruchinin S, Bogolubov NN, Adamenko S. Self-organization and nonequilibrium structures in the phase space. Int J Mod Phys B 2008;22:2025–45.
[14] Kitaura FS, Janka H-Th, Hillebrandt W. Explosions of O–Ne–Mg cores, the Crab supernova, and subluminous type II-P supernovae. Astron Astrophys 2006;450:345–50.
[15] Haines MG. An analytic model of radiative collapse of a Z-pinch. Plasma Phys Control Fusion 1989;31:759.
[16] Honda M, Meyer-ter-Vehn J, Pukhov A. Two-dimensional particle-in-cell simulation for magnetized transport of ultra-high relativistic currents in plasma. Phys Plasmas 2000;7:1302–8.
[17] Bret A, Firpo M-C, Deutsch C. Characterization of the initial filamentation of a relativistic electron beam passing through a plasma. Phys Rev Lett 2005;94:115002.
[18] Yonas G, Poukey JW, Prestwich KR, Freeman JR, Toepfer AJ, Clauser MJ. Electron beam focusing and application to pulsed fusion. Nucl Fusion 1974;14:731–40.
[19] Meger R, Commisso R, Cooperstein G, Goldstein S. Vacuum inductive store/pulse compression experiments on a high power accelerator using plasma opening switches. Appl Phys Lett 1983;42:943–5.
[20] Weber B, Commisso R, Meger R, Neri J, Oliphant W, Ottinger P. Current distribution in a plasma erosion opening switch. Appl Phys Lett 1984;45:1043–5.
[21] Neri J, Boller J, Ottinger P, Weber B, Young F. High-voltage, high-power operation of the plasma erosion opening switch. Appl Phys Lett 1987;50:1331–3.
[22] Lim J-W, Mimura K, Isshiki M. Application of glow discharge mass spectrometry for direct trace impurity analysis in Cu films. Appl Surf Sci 2004;227:300–5.
[23] Deeney C, Douglas MR, Spielman RB, Nash TJ, Peterson DL, L'Eplattenier P, Chandler GA, Seamen JF, Struve KW. Enhancement of X-ray power from a Z pinch using nested-wire arrays. Phys Rev Lett 1998;81:4883–6.
[24] VanDevender JP. Private communication, 2014.
[25] Cook DL, Allshouse GO, Bailey J, et al. Progress in light ion beam fusion research on PBFA II. Plasma Phys Control Fusion 1986;28:1921–30.
[26] Adamenko S, Adamenko A, Gurin A, Onishchuk Y. Track measurements of fast particle streams in pulsed discharge explosive plasma. Radiat Meas 2005;40:486489.
[27] Gurin AA, Adamenko AS, Adamenko SV, Kuzmenko MM. Proton- and α-radiation of the micro-pinch with the boron-containing target. Acta Polytechnica 2013;53:165–9.
[28] Freer M, Merchant AC. Developments in the study of nuclear clustering in light even–even nuclei. J Phys G 1997;23:261–324.
[29] von Oertzen W, Freer M, Kanada-En'yo Y. Nuclear clusters and nuclear molecules. Phys Rep 2006;432:43–113.
[30] Savage ME, Seidel DB, Mendel CW. Design of a command-triggered plasma opening switch for terawatt applications. IEEE Trans Plasma Sci 2000;28:1533–9.